SCIREA Journal of Materials
http://www.scirea.org/journal/Materials
March 19, 2023
Volume 8, Issue 1, February 2023
https://doi.org/10.54647/materials430216

EFFECT OF NiO AND CoO ADDITIVES ON CRYSTAL STRUCTURE AND MAGNETIC PROPERTIES IN MANUFACTURING MAGNETS $BaFe_{12}O_{19}$

Ramlan [1], Marzuki Naibaho [2], Endah Puspita[1], Yahri Seftiadi [1], Masno Ginting [2,*]

[1] Department of Physics, Faculty Science and Mathemathic, Sriwijaya University, South Sumatera 30862, Indonesia

[2] Research Center for Advanced Materials (PRMM), Nasional Research and Inovation Agency (BRIN), Serpong, South Tangerang, Indonesia

[*]Corresponding email: ramlan@unsri.ac.id

Abstrack

The synthesis of $BaFe_{12-2x}Co_xNi_xO_{19}$ (x = 0.5-1.5) at a calcination temperature of 1000°C using the coprecipitation method has been done by varying the concentration of the mixed precursor in order to identify the optimum sample. Barium Hexaferrite powder with 0.5% and 1% Nio-CoO has a $BaFe_{12}O_{19}$ phase. The DT-TGA curve analysis, at temperatures above 1000°C with a relatively small decrease in mass of 0.37%, indicates that the unwanted compounds have decomposed and the Barium Hexaferrite phase begins to form. Samples with a composition of 1%, NiO-CoO formed $BaFe_2O_4$ and NiBa phases, with a quantity of 96.4% $BaFe_2O_4$ phase. The phase change is caused by the lack of oxygen which weakening of the Fe-Sr-O bond. The magnetic properties of Barium Hexaferrite powder were successfully improved at 1% NiO-CoO, with a BHmax value of 2.26 MGOe.

Keyword: *$BaFe_{12}O_{19}$; Crystal Structure ; Magnetic Properties*

1. Introduction

Since the discovery of hexaferrite in 1950, this material has attracted great attention because of its potential use in miniaturization of electronic devices, which is the basic for the advances in electronic technology. Barium hexaferrite ($BaFe_{12}O_{19}$) is a ferrite-based magnetic material that has magnetic loss properties and large dielectric loss, high magnetization saturation, high conductivity and high temperature curie, and good chemical stability[1]–[4]. In addition, this Barium Hexaferrite material also has a relatively cheap price[5]. Furthermore, classical magnetic materials (i.e., metals) limit the miniaturization process due to their high density and weight. Due to its excellent magnetic properties and relatively low density, hexaferrite presents itself as a useful substitute for metals. They are currently used in applications such as permanent magnets, magnetic recording media, on-chip soft magnetic components, motor components, electrical generator, telecommunication devices, absorbent materials, sensors, microwave devices, military technology, automobiles, computers, radiation shielding, EMI devices, biomedical applications et al [6]–[11]. Barium Hexaferrite also have advantages such as low production costs, chemical stability, high coercivity, high Curie temperature (450°C) and resistance to corrosion [12], [13]. Many researchs had been done to engineer the hard magnetic properties of Barium Hexaferrite. To improve the magnetic properties of Barium hexaferrite, it is done by engineering the crystal structure of the material. One way to modify magnetic properties is by doping compounds with certain elements. Substitution or doping using divalent elements can change the magnetic properties of Barium Hexaferrite, because the elements of the group have almost the same ionic radius and electron configuration. Elements that are usually used as dopants are Mn, Ni, Co, Cu and Zn. Barium Hexaferrite nanomagnetic synthesis can be done by several methods including coprecipitation powder metallurgy[14], sol gel[15], ion exchange, auto combustion and so on[14][15][16]. Giordani et al., (2015) have conducted research related to doping by Ni and Co elements using the chemical coprecipitation method for type W hexaferrite. Fujiyati., (2018) has also conducted research related to Barium Hexaferrite doped using Ni and Co with x = 0; 0.1; 0.2 and 0.3 and Masno.,(2020) have also conducted research on barium hexaferrite using the coprecipitation method which was doped using Ni and Co with x=0, 0.1, and 0.2 with a temperature of 950^{o}C[2].

In this research it will be reported the barium hexaferrite doped by Ni and Co with three variations of composition x = 0.5; 1 and 1.5 using the powder metallurgy method with a combustion temperature of 1000^{o}C. The microstructure of the samples before and after heat treatment will be analyzed using Differential Thermal Analysis (DTA), X-Ray Diffractometer (XRD) and magnetic properties using a Vibrating Sample Magnetometer (VSM).

2. Experimental Procedure

The materials used in this study were $BaCO_3$ powder and α-Fe_2O_3 powder with a mole ratio of 1:6 and a total mass of 30 gr. In order to to determine each reactant mass used in the mixing process, the stoichiometric calculation should be done as shown in Table 1 below.

Table 1. Comparison of n (mol) and mass of raw materials.

Raw material	Mol	Mr (gr mol^{-1})	Mass (gr)
$BaCO_3$ Powder	1	197	5
$\alpha - Fe_2O_3$ Powder	6	160	25

Mixing $BaCO_3$ powder and α-Fe_2O_3 powder using a Rotary Ball Mill machine. Milling is carried out in wet milling conditions by adding 100 ml of distilled water as a lubricant, with the consideration of leaving 1/3 of the vial volume as empty space and a speed of 500 rpm. The Vial that was used with 8.5 cm in diameter and 10.5 cm in height made of ceramic material in order to avoid interaction with the vial walls during the milling process. The milling process was carried out for 6 hours, this milling time was based on the research of. Then the mixing in the form of lubricant was kept for about 16 hours in a glass container to separate the aquadest and milling powder. The milled powder that has settled in the container then dried using an oven at the temperature of 100^{o}C for about 5 hours. Furthermore, the dried milling powder crushed using a mortar pestle to get powder form.

After obtaining the mixed material $BaCO_3$ and α-Fe_2O_3 in powder form, then additives of NiO-CoO powder were added with a composition of 0.5%; 1%; 1.5% wt. Mixing is done using a mortar pestle. The Calcination of mixed powder is carried out in the oven at 1000^{0} C to form the crystallinity of the material. Then the characterizations carried out in this study are as follows: DTA-TGA test, using DTA type PT1600 brand Linseis, XRD (X-Ray Diffracton)

test, using XRD Rigaku SmartLab type 3 kW, VSM (Vibrating Sample Magnetometer) test, using VSM from Dexing Magnet Ltd type VSM250.

3. Result and Discussion

3.1. Thermogravimetric-Differential Thermal Analysis (TG-DTA)

The TG-DTA curve of the Barium Hexaferrite powder sample can be seen in Figure 1.

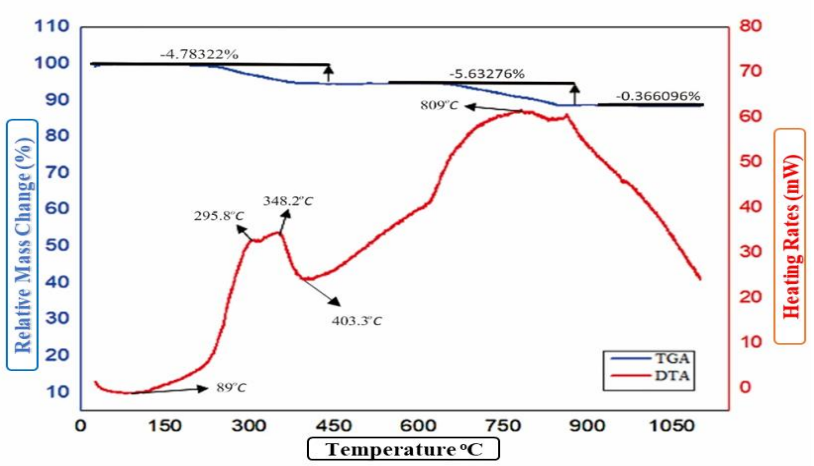

Figure 1. TG-DTA curve for Barium Hexaferrite magnetic powder.

From Figure 1 can be observed that the endothermic peak has been formed at a temperature of 89°C, this peak is associated with the release of the remaining free water content during the synthesis process. The decrease of sample mass occured at the temperature of about 250°C to 1000°C, with a total mass loss of up to 10.78%. At a temperature of 403.3°C indicates the release of CO_2 and water trapped in the pores. Two exothermic peaks were observed at 295.8°C and 348.2°C which can be seen on the DTA curve, these peaks indicate the possibility of crystallization of hematite and magnetite. At a temperature of 295.8°C as the peak of the formation of the hematite phase and the peak at 348.2°C as the magnetite phase with a mass reduction of 4.78322%. The next exothermic peak was at 809°C with a mass loss of 5.63%.

At a temperature of 800°C - 900°C it is susceptible to the formation of a secondary oxide phase ($BaFe_2O_4$), so that the expected hexaferrite phase is not fully formed at that temperature and will result in lower remanance (Mr) and coercivity (Hc) values and reduce the magnetic quality of the synthesized material. Based on the TG-DTA curve, the characterization results detected that a relatively small mass decrease reached 0.366094% which could be stated that

the Barium Hexaferrite ($BaFe_{12}O_{19}$) phase began to form at a temperature of ≥900°C. Due to the limitations of the analyzer which only detects up to 1100°C, the sample combustion in this study uses a temperature of 1000°C.

3.2. X-Ray Diffraction (XRD)

The X-ray diffraction pattern on Barium Hexaferrite powder sample can be seen in Figure 2.

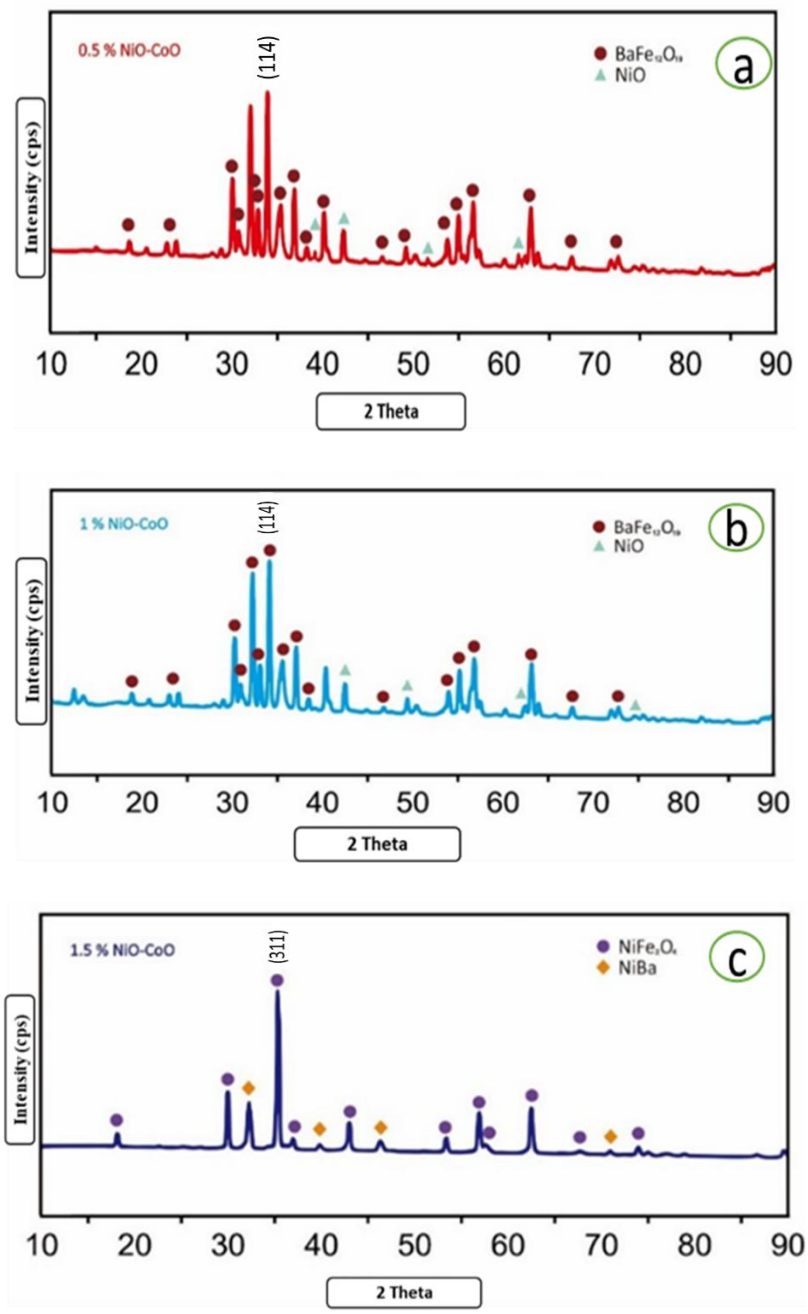

Figure 2. X-ray diffraction pattern on Barium Hexaferrite powder with variations in dopant composition

The diffraction pattern of XRD test results on samples with variations in NiO-CoO (0.5%; 1% and 1.5%) can be seen in Figure 2. The xrd test results of Barium Hexaferrite powder with 0.5% Ni-CoO (figure 2a) showed that the sample had a $BaFe_{12}O_{19}$ phase and with a small number NiO phases were detected. Then the analysis was carried out on Barium Hexaferrite powder which was added with 1% NiO-CoO (figure 2b). The results showed that the sample also had a $BaFe_{12}O_{19}$ phases and with a small number NiO as well as Barium Hexaferrite with doped (0.5% NiO-CoO). The absence of CoO additives detected in the 0.5% and 1% NiO-CoO Barium Hexaferrite powder can be stated that the Co^{+2} ions were successfully substituted into the crystal structure of the sample [17]. The smaller Co^{+2} ion caused its presence to be undetected and succeeded in replacing the position of the Fe^{+3} ion [18][19], so that no foreign phase other than $BaFe_{12}$ O_{19} was detected during the test. In the sample with the addition of 1.5% NiO-CoO (figure 2c), the formed phase was not $BaFe_{12}O_{19}$ but became two different phases. The diffraction pattern that has gone through the analysis process was detected that the formation of Barium Monoferrite ($BaFe_2O_4$) and NiBa phases was detected. For the sample with 1.5% NiO-CoO, the quantity of $BaFe_2O_4$ formed was 94.4% and the remaining 5.6% was NiBa phase. The appearance of these two phases ($BaFe_2O_4$ and NiBa) is probably caused by oxygen deficiency or oxygen deficiency events during combustion. This event makes the compound reaction and the bond between Fe-Ba-O that occur is not perfect. As a result, there is a weakening of the oxygen ion bond with other ions and a vacancy occurs at the oxygen ion position. The Ni^{+2} ion gets a bigger opportunity along with the increasing number of additives that are substituted in the crystal structure of the sample, thereby replacing, and filling the vacancy due to the release of oxygen ions. As well as causing a reaction to ferrite and produce a dominant phase $BaFe_2O_4$. A small portion of the other Ni^{+2} ions will bind to Ba^{+2} ions which then form the NiBa phase.

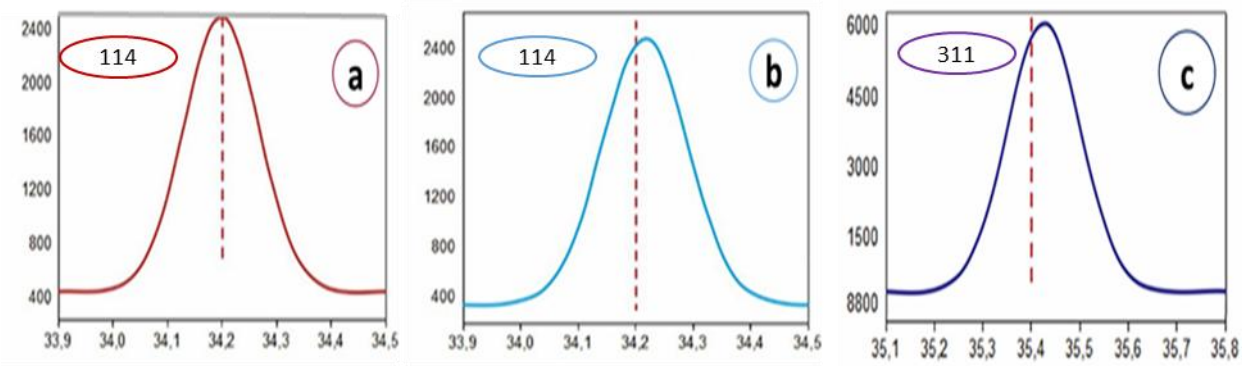

Figure 3. Graph of shift in the diffraction pattern at the highest intensity (a) for 0.5% NiO-CoO (b) for 1% NiO-CoO and (c) for 1.5% NiO-CoO.

The position of the diffraction pattern on Barium Hexaferrite with 0,5% NiO-CoO variation represented by the diffraction peak at the highest intensity experienced an angle shift to the Barium Hexaferrite peak with 1% NiO-CoO variation. The shift occurs to the right which can be observed in Figure 3(a) and 3(b) above. The highest peak of Barium Hexaferrite 0.5% NiO-CoO with a plane (114) at an angle of 34.23°. The angle shift that occurs is 0.04° in Barium Hexaferrite with 1% NiO-CoO with the highest peak at an angle of 34.27°. For NiO-CoO composition of 1.5%, the highest peak in the plane (311) is at an angle of 35.43°. This change in position or shift is due to the difference between the radii of the Ni^{+2} and Ba^{+2} ions. The radius of the Ni^{+2} ion is 0.69 A and the Ba^{+2} ion has a radius of 1.42 A. If the radius of the substituted ion is larger than the Ba^{+2} ion, the cell volume, lattice parameters and crystal structure widening will be even greater [17][20]. It is known that the radius of the Ni^{+2} ion is smaller than that of the Ba^{+2} ion which causes the lattice parameters and cell volume of the samples synthesized in this study to be smaller, this change can be observed in table 2. Therefore, the distance between the crystal planes will also experience narrowing or getting smaller. According to Bragg's law, the distance between planes of atoms is inversely proportional to the diffraction angle[21]. The smaller the distance between the crystal planes, the greater the diffraction angle and vice versa. Based on this, it can be stated that the shift in the position of the diffraction peak of the sample towards a larger angle along with the increase in substitution of the number of Ni^{+2} ions in this study was caused by the smaller radius of the substituted Ni^{+2} ion.

Table 2 Value of lattice parameters and size of Barium Hexafrite powder with NiO-CoO additive.

Name Sample	**Composition $NiO - CoO$ (%)**	**Lattice Constant**			**Crystal Size (nm)**
		a ($\dot{A}$)	c ($\dot{A}$)	c/a	
A	0,5	5,8650	23,0990	3,93845	67 ± 0,34
B	1	5,8930	23,1940	3,98585	80,7 ± 0,18
C	1,5	8,4067	8,4067	1	88,75 ± 0,59

Table 2. above contains several quantities of XRD parameters analyzed using the Match. Which include lattice constants and cell volume and crystal size calculated using the Scherrer method. Barium Hexaferrite with 0.5% NiO-CoO has a lattice constant (a= 5.8650 $\dot{A}$; c= 23.0990 $\dot{A}$)) which is smaller than Barium Hexaferrite with 1% dopant composition with a value of (a = 5.8930 $\dot{A}$; c = 23.1940 $\dot{A}$). For samples with a composition of 1.5% also experienced a decrease in the value of the lattice constant and cell volume. The c/a ratio

(height and width ratio) can be used to determine the crystal structure. The c/a ratio which is close to 3.98 indicates the material is a type M ferrite with a hexagonal structure [22]. Barium Hexaferrite with 0.5% and 1% NiO-CoO has a c/a ratio of 3.93845 and 3.98585, respectively. So, it can be stated that both have a hexagonal crystal structure. Meanwhile, the 1% NiO-CoO composition produced $BaFe_2O_4$ phase with a cubic crystal structure. The sample with the addition of NiO-CoO has a smaller crystal size than pure Barium Hexaferrite, this is because the Ni^{+2} ion which is substituted during synthesis inhibits crystal growth and leads to a decrease in crystal size[23]. The resulting crystal size based on calculations using the Scherrer method for 0.5% and 1% NiO-CoO increased from 67 nm to 80.7 nm. Meanwhile, Barium Hexaferrite with 1.5% NiO-CoO produces crystals with a size of 88.75 nm.

3.3. Vibrating Sample Magnetometer (VSM)

To observe changes in the size of the hysteresis curve caused by the addition of an additive in the form of NiO-CoO powder with several variations in composition, it can be observed in Figure 4.

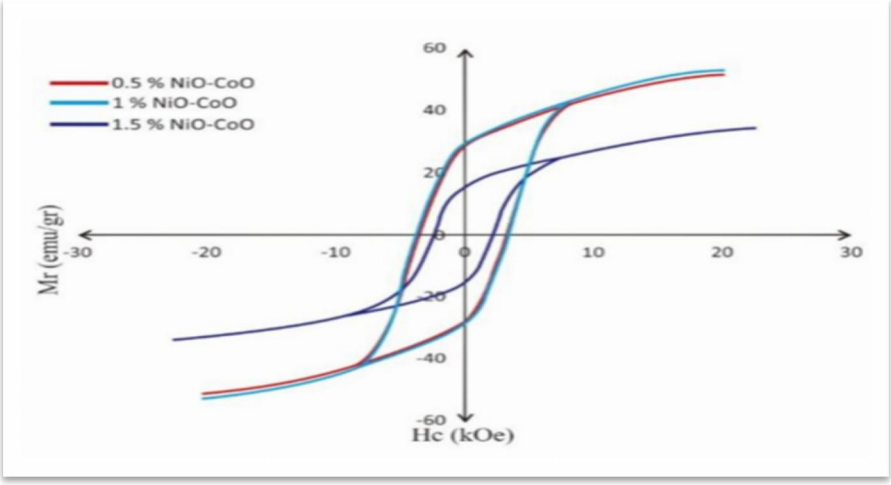

Figure 4. Barium Hexaferrite hysteresis curve with various additives.

Figure 4. shows the barium hexaferrite hysteresis curve with the addition of 0.5% additive (NiO-CoO). The results of the curve analysis that have been carried out show that the magnetic saturation value (Ms) of pure Barium Hexaferrite is 3.901 emu/gr, remanence (Mr) is 2.2 emu/gr, coercivity (Hc) is 3.437 kOe. From this information, it is known that the coercivity of Barium Hexaferrite with 0.5% doping is greater than 200 Oe. So that the Barium Hexaferrite powder which produces a single $BaFe_{12}O_{19}$ and NiO can be classified as a permanent magnet [22].

The results of the test and analysis of the quantity parameters on the hysteresis curve as a representation of the magnetic properties of sample B (1% NiO-CoO) obtained the value of Ms = 52.93 emu/gr; Mr = 29.69 emu/gr and Hc = 3.617 kOe. When compared between samples A and B, an increase in the magnetic properties that occurs in sample B. Magnetic properties of Barium Hexaferrite comes from Fe3+ ions which are distributed as many as 24 ions [20] at positions 12k, 2a, 2b with spin up and 4f1, 4f2 with spin down. Thus, the total magnetic moment depends on the number of spin ups and spins down on the material [17]. In one BaFe12O19 unit cell there are 8 spin downs and 16 spin ups which produce a total magnetic moment of 40μB, with a magnetic moment of Fe^{3+} ion of 5μB [23]. Barium Hexaferrite with the addition of 1% which has been synthesized produces a single phase of $BaFe_{12}O_{19}$ without the presence of a foreign phase, this indicates that the Mg+2 ion has been successfully substituted into the crystal structure of $BaFe_{12}O_{19}$.

The results of the VSM test that had been carried out on sample C or Barium hexaferrite powder with 1.5% NiO-CoO resulted in a hysteresis curve as shown in Figure 4. Analysis of the curve readings resulted in the value of Ms = 34.53 emu/gr; Mr = 15.69 emu/gr and Hc = 2.186 kOe. NiO-CoO powder which was substituted to Barium Hexaerite powder as much as 1.5% produced a composite phase in the form of $BaFe_2O_4$ (magnetic) and NiBa (non-magnetic) with cubic crystal structure. The magnetic properties of sample C decreased because the dominant phase ($BaFe_2O_4$) only had a total magnetic moment of about 1 to 2.2μB [23] lower than $BaFe_{12}O_{19}$ in samples A and B. [24]. To observe changes in the size of the hysteresis curve caused by the addition of additives in the form of MgO powder with several variations in composition, it can be observed in Figure 4.

Maximum product energy (BH)max as one of the parameters used to review the magnetic properties of materials in addition to remanence, coercivity and saturation. The value (BH)max of a material can be determined based on the curve in quadrant II. Hysteresis curves in quadrant II for samples A, B and C can be observed in Figure 5 along with the quantity of magnetic parameters shown in Table 3. The remanence unit on the curve has been converted from emu/gr to gauss (Attached).

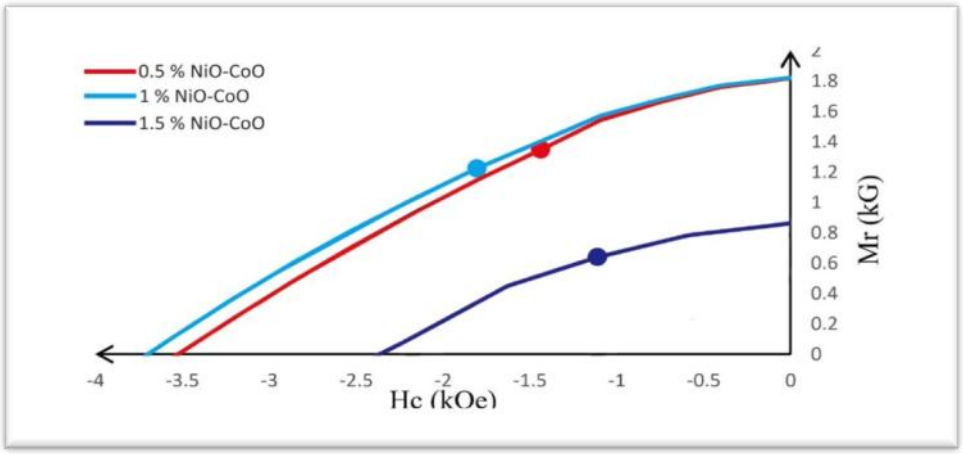

Figure 5. Hysteresis curve of samples A, B and C in quadrant II.

Tabel 3. Magnetic properties of Barium Hexaferrite with variations in the composition of NiO-CoO.

Sample	Composition of $Nio - CoO$ (%)	M_r (emu/gr)	Hc (kOe)	M_s (emu/gr)	$\frac{Mr}{Ms}$	BHmax (MGOe)
A	0,5	28,47	3,437	53,49	0,53	2,07
B	1	29,69	3,617	52,93	0,56	2,22
D	1,5	15,69	2,186	34,53	0,45	0,74

It can be observed in Table 3 that the coercivity values of samples A, B, and C are higher than 200 Oe, this indicates that all the magnetic powders that have been synthesized are permanent magnets [19]. In sample B (1% MgO) the value of (BH)max was successfully increased compared to sample A from 2.07 MGOe to 2.22 MGOe. Increasing the magnetization saturation of the powder by 1.5%; NiO occurs due to an increase in the quantity of the magnetic phase ($BaFe_2O_4$) of 94.4%. As previously explained, there was a decrease in the remanence and coercivity values in the sample with 1.5% additives due to the change in the phase of the material, which resulted in a decrease in the value of (BH)max. Although the phase in sample C formed was not as expected, in the industrial field the magnetic powder can be used in various applications such as data storage media and as permanent magnets. This is because the remanance (Mr)/saturation(Ms) ratio of the sample is in the interval 0.2 – 0.59[24].

4. Conclusion

Based on the data and analysis of the research that has been done, it can be concluded that:

Based on the DT-TGA curve analysis, at temperatures above 1000^{o}C with a relatively small decrease in mass of 0.37%, it indicates that the unwanted compounds have decomposed and the Barium Hexaferrite phase begins to form. Barium Hexaferrite powder with 0.5% and 1% Nio-CoO has a $BaFe_{12}O_{19}$ phase and with a small number NiO phases were detected. Samples with a composition of 1,5%, NiO-CoO formed $BaFe_2O_4$ and NiBa phases, with a quantity of 96.4% $BaFe_2O_4$ phase. The phase change is caused by a lack of oxygen and causes a weakening of the Fe-Ba-O bond. The magnetic properties of Barium Hexaferrite powder were successfully improved at 1% NiO-CoO, with a BHmax value of 2.26 MGOe. So this sample is very suitable for the manufacture of permanent magnets.

REFERENCE

[1] E. Handoko et al., "Microwave absorption performance of barium hexaferrite multi-nanolayers," Mater. Express, vol. 10, no. 8, pp. 1328–1336, 2020, doi: 10.1166/mex.2020.1811.

[2] M. Ginting et al., "Effect of Co and Ni additions as doping materials on the micro-structures and the magnetic properties of barium hexa-ferrites," Case Stud. Therm. Eng., vol. 18, p. 100589, 2020, doi: 10.1016/j.csite.2020.100589.

[3] J. Edianta, N. Fauzi, M. Naibaho, F. S. Arsyad, and I. Royani, "Review of the effectiveness of plant media extracts in barium hexaferrite magnets (Bafe12o19)," Sci. Technol. Indones., vol. 6, no. 2, pp. 39–52, 2021, doi: 10.26554/STI.2021.6.2.39-52.

[4] D. Chen, Y. Liu, Y. Li, K. Yang, and H. Zhang, "Microstructure and magnetic properties of Al-doped barium ferrite with sodium citrate as chelate agent," J. Magn. Magn. Mater., vol. 337–338, pp. 65–69, 2013, doi: 10.1016/j.jmmm.2013.02.036.

[5] S. Anand, S. Pauline, and C. J. Prabagar, "Zr doped Barium hexaferrite nanoplatelets and RGO fillers embedded Polyvinylidenefluoride composite films for electromagnetic interference shielding applications," Polym. Test., vol. 86, no. March, p. 106504, 2020, doi: 10.1016/j.polymertesting.2020.106504.

[6] S. Gupta, S. K. Deshpande, V. G. Sathe, and V. Siruguri, “Effect of scandium substitution on magnetic and transport properties of the M-type barium hexaferrites,” J. Alloys Compd., vol. 815, p. 152467, 2020, doi: 10.1016/j.jallcom.2019.152467.

[7] R. Ramlan, P. Sardjono, M. Muljadi, D. Setiabudidaya, and F. Gulo, “Analysis of the physical, mechanical, and magnetic properties of hard magnetic composite materials NdFeB made using bakelite polymers,” J. Magn., vol. 24, no. 1, pp. 39–42, 2019, doi: 10.4283/JMAG.2019.24.1.039.

[8] V. Pratap, A. K. Soni, S. M. Abbas, A. M. Siddiqui, and N. E. Prasad, “Effect of zinc substitution on U-type barium hexaferrite-epoxy composites as designed for microwave absorbing applications,” J. Alloys Compd., vol. 865, p. 158280, 2021, doi: 10.1016/j.jallcom.2020.158280.

[9] C. P. Granja-Banguera, D. G. Silgado-Cortázar, and J. A. Morales-Morales, “Transition Metal Substituted Barium Hexaferrite-Modified Electrode: Application as Electrochemical Sensor of Acetaminophen,” Molecules, vol. 27, no. 5, 2022, doi: 10.3390/molecules27051550.

[10] B. da Costa Andrade and M. A. Macêdo, “Structural and magnetoelectric properties of a new w-type hexaferrite (Sr0.85Ce0.15Co2Fe16O27-Δ),” Adv. Mater. Res., vol. 975, pp. 263–267, 2014, doi: 10.4028/www.scientific.net/AMR.975.263.

[11] J. Y. Kim et al., “Enhancement of adhesion between polyphenylene sulfide and copper by surface treatments,” Curr. Appl. Phys., vol. 14, no. 1, pp. 118–121, 2014, doi: 10.1016/j.cap.2013.10.015.

[12] Ramlan, Muljadi, P. Sardjono, D. Setiabudidaya, and F. Gulo, “Influence of addition Ba-Ferrite on the hardness, magnetic properties and corrosion resistance of hybrid bonded magnet NdFeB,” J. Phys. Conf. Ser., vol. 1204, no. 1, 2019, doi: 10.1088/1742-6596/1204/1/012013.

[13] S. Verma et al., “Understanding the phase evolution with temperature in pure (BaFe12O19) and zinc-zirconium co-doped barium hexaferrite (BaZnZrFe10O19) samples using Pawley and Rietveld analysis,” Mater. Today Commun., vol. 27, no. April, p. 102291, 2021, doi: 10.1016/j.mtcomm.2021.102291.

[14] Ramlan, D. Setiabudidaya, Suprapedi, A. A. Bama, and Muljadi, “Study on the effect of CaO addition on micro structure and magnetic properties of BaFe12O19 made using powder metallurgy technique,” AIP Conf. Proc., vol. 2221, 2020, doi: 10.1063/5.0003036.

[15] M. Chandel et al., “Fabrication of Ni2+ and Dy3+ substituted Y-Type nanohexaferrites: A study of structural and magnetic properties,” Phys. B Condens. Matter, vol. 595, p. 412378, 2020, doi: 10.1016/j.physb.2020.412378.

[16] J. Mohammed et al., “Crystal structure refinement and the magnetic and electro-optical properties of Er3+–Mn2+-substituted Y-type barium hexaferrites,” Ceram. Int., vol. 47, no. 13, pp. 18455–18465, 2021, doi: 10.1016/j.ceramint.2021.03.169.

[17] T. T. Carol, J. Mohammed, B. Hamid, S. Mishra, S. Kumar, and A. K. Srivastava, “Effect of Cr – Bi Substitution on The Structural, Optical, Electrical and Magnetic Properties of Strontium Hexaferrites,” Phys. B Phys. Condens. Matter, vol. 575, p. 411681, 2019, doi: 10.1016/j.physb.2019.411681.

[18] I. Ramli, I. N. Saidah, F. R. S, and M. Zainuri, “Pengaruh Variasi pH Pelarut HCl Pada Sintesis Barium M-Heksaferrit dengan Doping Zn (BaFe11,4Zn0,6O19) Menggunakan Metode Kopresipitasi,” J. Sains dan Seni ITS, vol. 1, no. 1, pp. 41–46, 2012.

[19] Z. E. Senida, Ramli, Ratnawulan, and Hidayati, “Pengaruh Variasi Komposisi MnFe2O4 Terhadap Sifat Magnetik Nanokomposit MnFe2O4 / PANi yang Disintesis dengan Metoda Sol – Gel Spin Coating Mahasiswa Pendidikan Fisika , FMIPA Universitas Negeri Padang Staf Pengajar Jurusan Fisika , FMIPA Universita,” Pillar Phys., vol. 12, pp. 17–24, 2019.

[20] M. Khandani, M. Yousefi, S. S. S. Afghahi, M. M. Amini, and M. B. Torbati, “An Investigation of Structural and Magnetic Properties of Ce – Nd Doped Strontium Hexaferrite Nanoparticles as A Microwave Absorbent,” Mater. Chem. Phys., vol. 235, p. 121722, 2019, doi: 10.1016/j.matchemphys.2019.121722.

[21] Y. Iriani, L. Setyaningsih, and A. Jamaluddin, “Analisis pengaruh variasi dopan lantanum terhadap struktur kristal dan morfologi lapisan tipis barium strontium titanat,” Indones. J. Appl. Phys., vol. 2, no. 2, pp. 170–175, 2012.

[22] S. K. Chawla, S. S. Meena, P. Kaur, R. K. Mudsainiyan, and S. M. Yusuf, “Materials Effect of Site Preferences on Structural and Magnetic Switching Properties of CO – Zr

Doped Strontium Hexaferrite SrCo x Zr x Fe (12 À 2 x) O 19," J. Magn. Magn. Mater., vol. 378, pp. 84–91, 2015, doi: 10.1016/j.jmmm.2014.10.168.

[23] A. U. Rasyid, P. Southern, J. A. Darr, S. Awan, and S. Manzoor, "Strontium Hexaferrite (SrFe12O19) Based Composites for Hyperthermia Applications," J. Magn. Magn. Mater., vol. 344, pp. 134–139, 2013, doi: 10.1016/j.jmmm.2013.05.048.

[24] S. Ghezelbash, M. Yousefi, M. Hossainisadr, and S. Baghshahi, "Structural and Magnetic Properties of Sn4+ Doped Strontium Hexaferrites Prepared via Sol–Gel Auto-Combustion Method," IEEE Trans. Magn., pp. 1–6, 2018, doi: 10.1109/TMAG.2018.2844364.